Supporting Information

Two-dimensional Be_2P_4 as promising thermoelectric material and anode for Na/K-ion batteries

Nidhi Verma, Poonam Chauhan and Ashok Kumar*

Department of Physics, Central University of Punjab, Bathinda, India-151401

(July 3, 2024)

*Corresponding Author: ashokphy@cup.edu.in

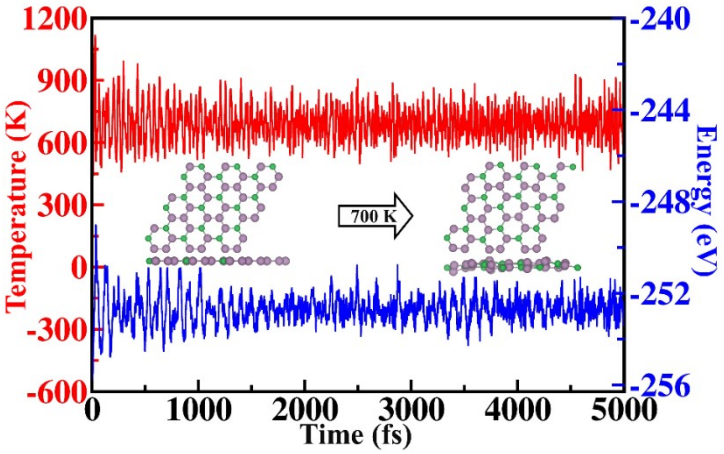

Figure S1: MD simulation energy and temperature profiles of Be_2P_4 concerning time steps for 700 K temperature. The inset additionally displays the initial and final structures of monolayer following the 5000 fs.

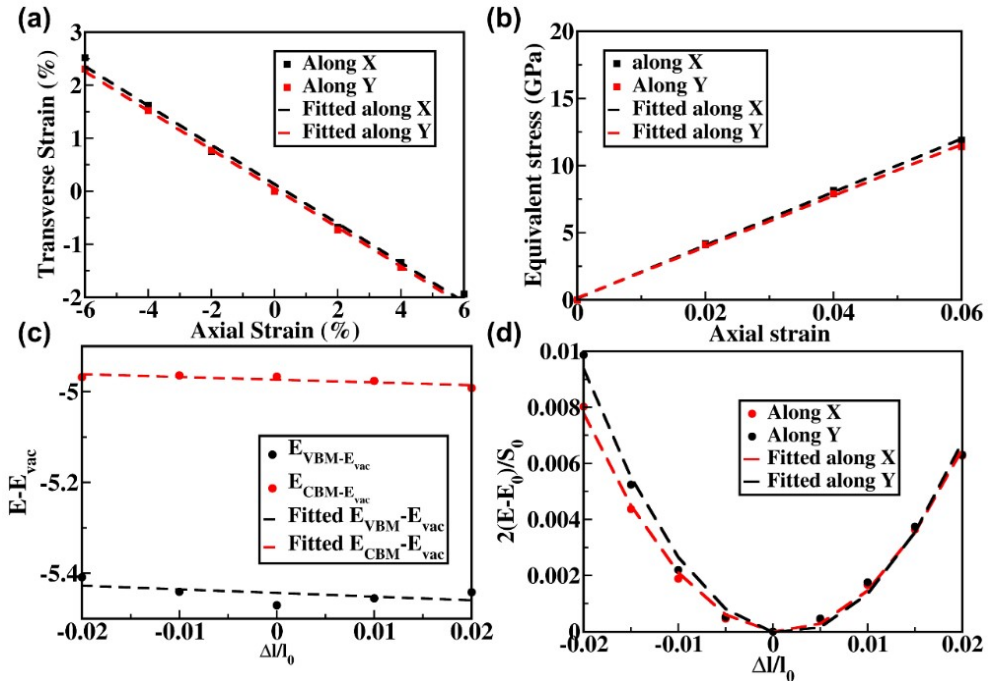

Figure S2: (a) Transverse strain **(b)** Equivalent stress as a function of axial strain along the x- and y-axis. **(c)** Graph and straight fit graph between $E - E_{vac}$ and $\frac{\Delta l}{l_0}$ along x and y axis, $E - E_{vac}$ is the energy difference of i[th] band and vacuum energy, $\frac{\Delta l}{l_0}$ is the strain in the respective direction. **(d)** Graph and parabolic fit between $\frac{(2E - E_0)}{S_0}$ and $\frac{\Delta l}{l_0}$; $(2E - E_0)$ is the

difference in the total energy of unstrained and strained structure, S_0 is the surface area of Be_2P_4 monolayer and $\frac{\Delta l}{l_0}$ is the strain in the corresponding direction.

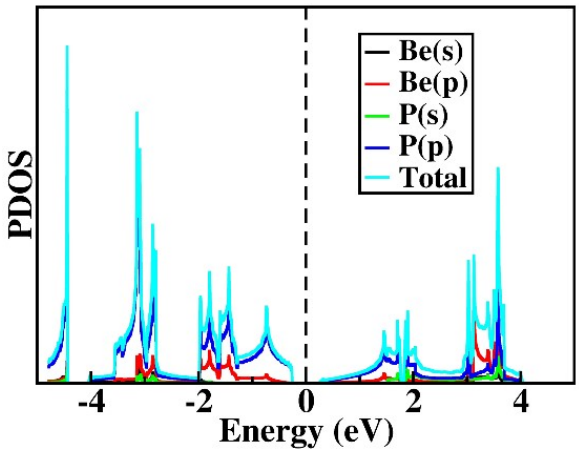

Figure S3: The projected density of state (PDOS) using the GGA+PBE level of theory.

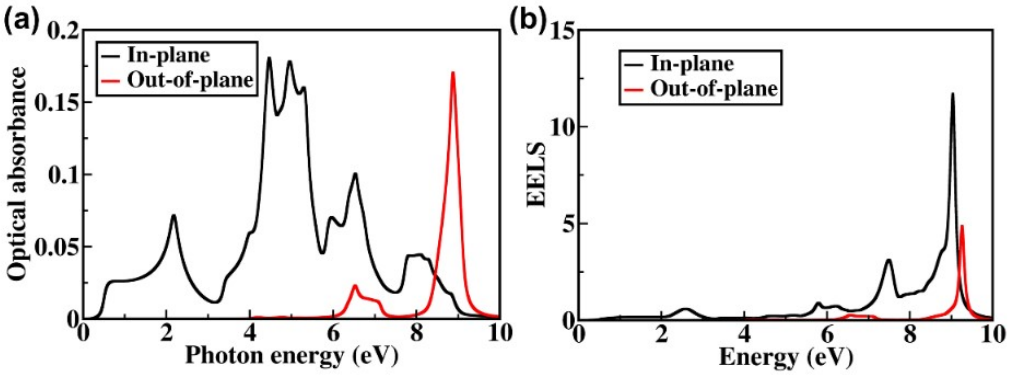

Figure S4: (a) Optical absorbance **(b)** electron energy loss spectrum (EELS) of Be_2P_4 monolayer using GGA+PBE method.

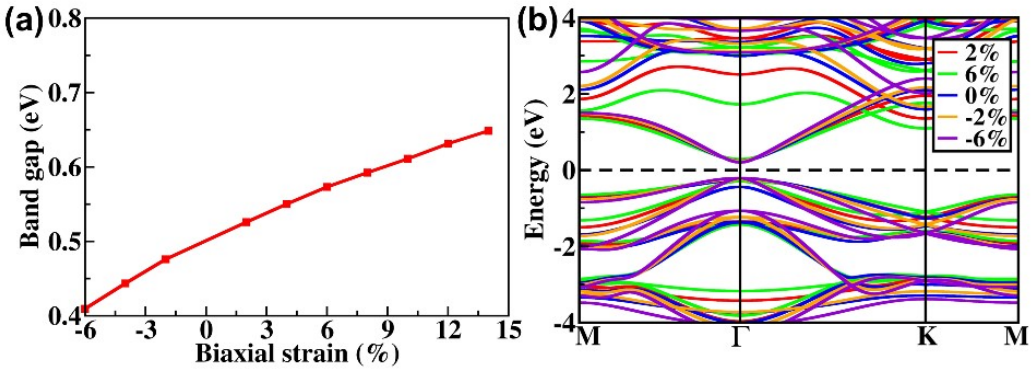

Figure S5: (a) Band gap variation **(b)** electronic band structure of Be_2P_4 monolayer corresponding to different biaxial strains using GGA+PBE method.

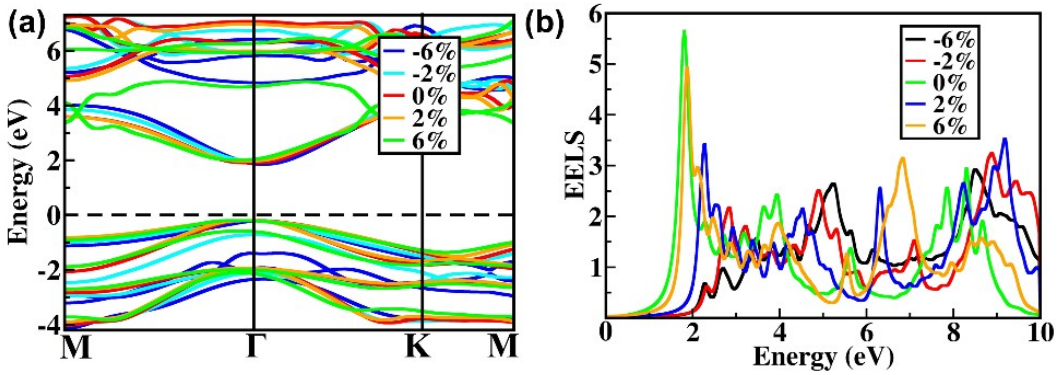

Figure S6: (a) Electronic band structure **(b)** Electron energy loss spectra of Be_2P_4 monolayer corresponding to different biaxial strains using GW+BSE method.

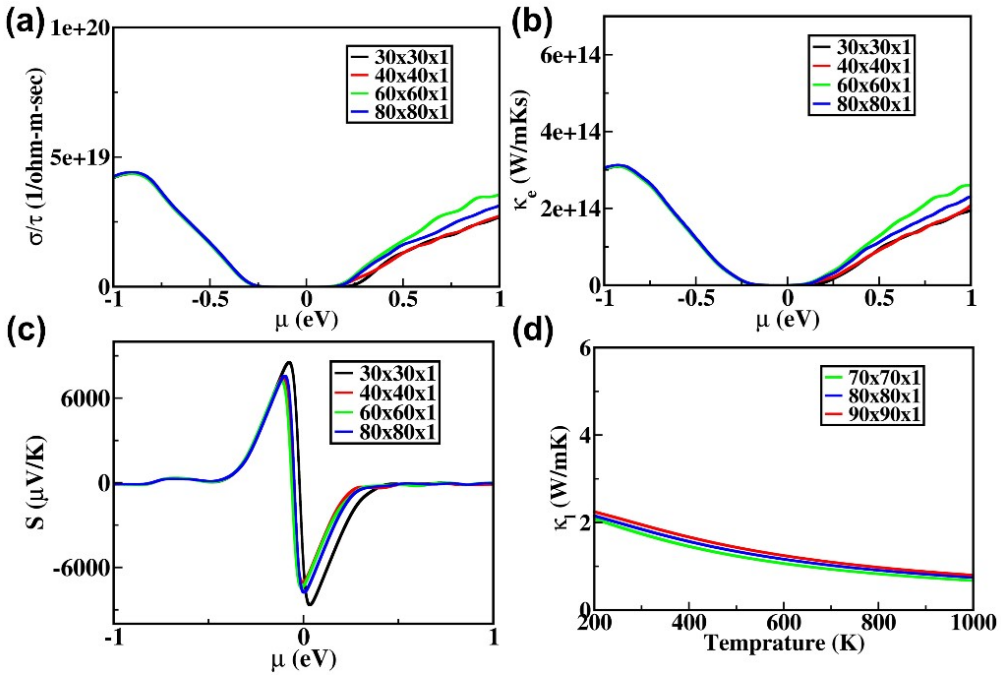

Figure S7: Convergence test plot of **(a)** electrical conductivity, **(b)** electronic thermal conductivity **(c)** Seebeck coefficient and **(d)** Lattice thermal conductivity.

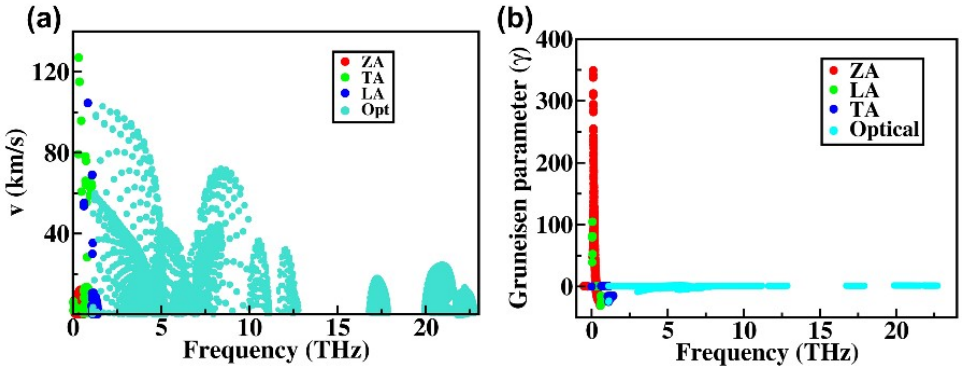

Figure S8: (a) group velocity (ν) and **(b)** Gruneisen parameter (γ) plot with respect to frequency of Be_2P_4 monolayer.

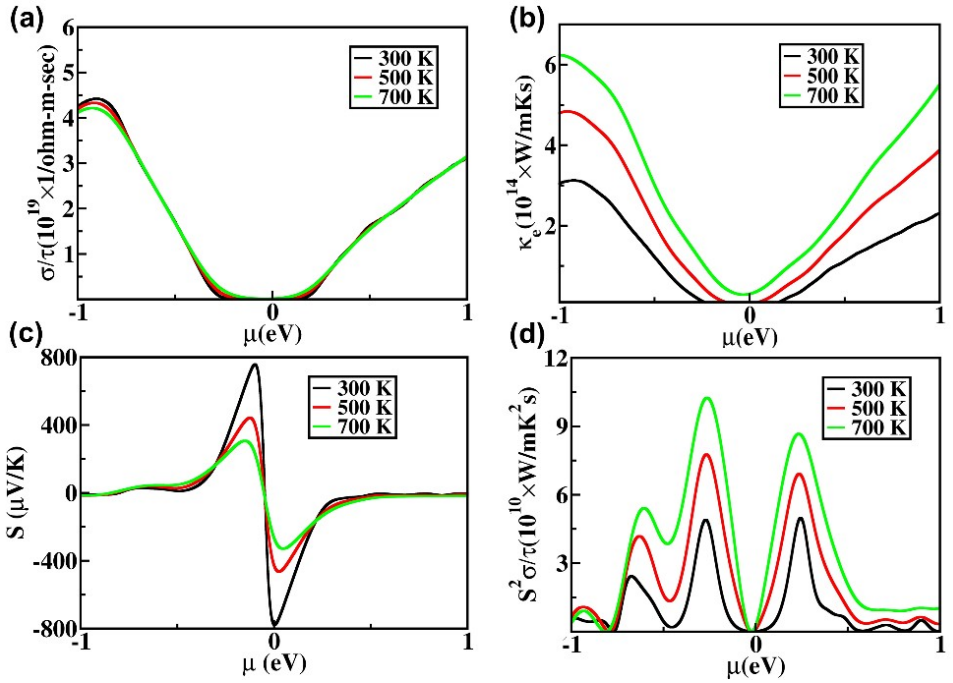

Figure S9: (a) Electrical conductivity, **(b)** electronic thermal conductivity **(c)** Seebeck coefficient and **(d)** power factor of Be_2P_4 monolayer corresponding to different temperature.

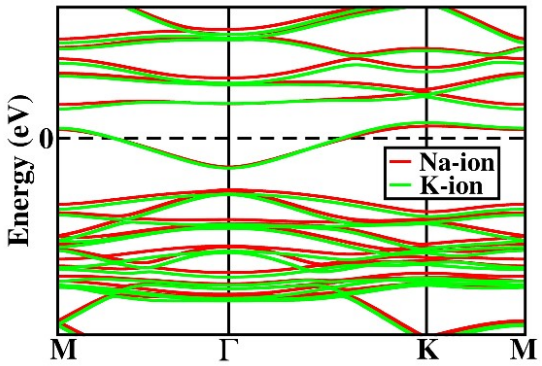

Figure S10: Electronic band structure of Be_2P_4 monolayer after adsorption of single Na and K-atoms.

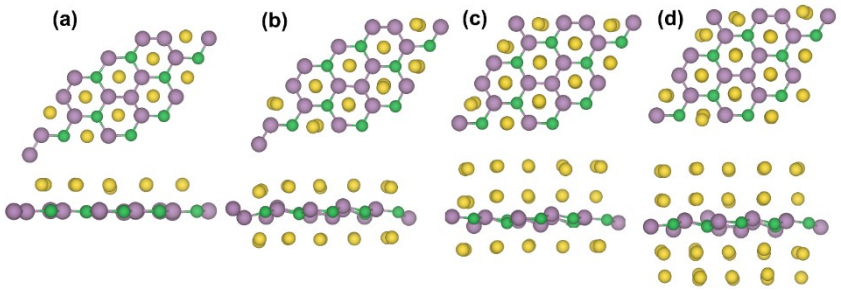

Figure S11: Top and side view of Be_2P_4 monolayer during the adsorption of Na-atoms layer. The green, vine and yellow colour balls represent Be, P and Na atoms, respectively.

Table 1: A comparative analysis of anodic performance of previously studied 2D materials.

Sr. No.	**Anode materials**	**Diffusion barrier (eV)**	**Open circuit voltage (V)**	**Specific capacity (mAh/g)**	**Energy density (Wh/Kg)**	**References**
1.	Be_2P_4 (Na/K)	0.23/0.18	0.8/0.1	3776.93/3021.55	8460.32/8883.35	This work*
2.	Be_2P_3N (Na/K)	0.06/0.04	0.02/0.1	2574/1716	5055/ 3325	[1]
3.	o-B_2N_2 (Na)	0.16	0.33	2159.83	-	[2]
4.	Θ-graphene	0.39/0.22	0.29/0.60	1275.12/956.34	-	[3]
5.	BeN_4 (K)	0.06	0.179–0.084	842	-	[4]
6.	B_2P_2 (Na/K)	0.10/0.07	0.26/0.47	1282.34/854.89	-	[5]
7.	BC_3(Na/K)	-	0.12/0.16	572/858	-	[6]
8.	Penta siligraphene (Na/K)	-	-	514.3/1028.7	-	[7]

9.	Penta-diamond (Na/K)	0.25/0.10	0.33/0.80	2231.49/743.86	-	[8]
10.	Be_2C_5 (K)	0.074	0.28	2060	5455	[9]

References:

1. Sun, S. and X. Ye, *Monolayer Be2P3N as a high capacity and high energy density anode material for ultrafast charging Na-and K-ion batteries.* Applied Surface Science, 2020. **527**: p. 146783.
2. Khossossi, N., et al., *Revealing the superlative electrochemical properties of o-B2N2 monolayer in Lithium/Sodium-ion batteries.* Nano Energy, 2022. **96**: p. 107066.
3. Wang, S., et al., *Reconfiguring graphene for high-performance metal-ion battery anodes.* Energy Storage Materials, 2019. **16**: p. 619-624.
4. Cheng, Z., et al., *BeN4 monolayer as an excellent Dirac anode material for potassium-ion batteries.* Journal of Alloys and Compounds, 2023. **936**: p. 168351.
5. Lin, H., et al., *Flexible borophosphene monolayer: A potential Dirac anode for high-performance non-lithium ion batteries.* Applied Surface Science, 2021. **544**: p. 148895.
6. Joshi, R.P., et al., *Hexagonal BC3: A robust electrode material for Li, Na, and K ion batteries.* The Journal of Physical Chemistry Letters, 2015. **6**(14): p. 2728-2732.
7. Wang, H., et al., *Two-dimensional penta-siligraphene with high performance for non-lithium metal ions batteries anode materials.* Solid State Ionics, 2022. **385**: p. 116020.
8. Younis, U., et al., *Two-dimensional metallic pentadiamond as anode material for Li-/Na-/K-ion batteries with high performance.* Materials Today Energy, 2021. **20**: p. 100664.
9. Wang, F., et al., *Be 2 C 5 Monolayer with Quasiplanar Pentacoordinate Carbon Atoms and Ultrahigh Energy Density as a Dirac Anode for Potassium-Ion Batteries.* PRX Energy, 2023. **2**(3): p. 033012.